Analysis of NMR and conductivity-relaxation measurements in glassy Li_2S-SiS_2 fast-ion conductors

K. L. Ngai
Naval Research Laboratory, Washington, D.C. 20375-5232
(Received 12 March 1993)

^{7}Li nuclear spin-lattice relaxation (NSR) and Li-ion electrical-conductivity relaxation (ECR) data of $(Li_2S)_{0.56}(SiS_2)_{0.44}$, a glassy fast-ionic conductor, have been reanalyzed. Both NSR and ECR data are fitted by using a stretched exponential, $\exp[-(t/\tau^*)^\beta]$, for the correlation function in each relaxation. It is found that τ_s^* for NSR can be several orders of magnitude longer than τ_σ^* for ECR at the same temperature, β_s and β_σ are not the same with $\beta_s < \beta_\sigma$, and the activation energy E_s^* of τ_s^* is significantly larger than E_σ^* of τ_σ^*. In this contribution we show how these pronounced differences of the parameters in the correlation functions of NSR and ECR are explained in the framework of the coupling model. An additional predicted relation: $\beta_s E_s^* = \beta_\sigma E_\sigma^*$ is found to be consistent with the experimental data and the common value of the two products is identified naturally with the true single ion activation energy. The constraints that these experimental data impose on any viable theory of the dynamics of carriers in glassy ionic conductors are discussed.

INTRODUCTION

Nuclear spin relaxation (NSR) and electrical-conductivity relaxation (ECR) measurements are the two techniques[1–19] most often used to probe the motion of ionic charge carriers in fast-ion conductors. The ultimate goal of these measurements is to find out the exact nature of the dynamics of the ionic charge carriers in transport. As has happened before in other problems of scientific research, critical experimental facts are needed to identify which, among possible theories and models, is the correct one. An example of such a critical experimental fact is the anomalous Li isotope mass dependence observed[19] in $Li_2O(B_2O_3)_3$ glasses. Another example is the recently found pronounced differences between the NSR correlation time and the conductivity relaxation times in a Li chloroborate glass $(LiCl)(Li_2O)(B_2O_3)_2$ by Tatsumisago, Angell, and Martin.[14] They found their conductivity relaxation at a certain fixed temperature occurs on a time scale longer by two orders of magnitude than the ^{7}Li NSR relaxation, and has a significantly lower activation energy. Similar differences can be identified in other glassy ionic conductors,[14,15,18] and in Na β-alumina,[20] indicating that this discrepancy is real and general. Similar conclusions have been drawn also from Monte Carlo simulation of ions moving in a disordered environment.[21]

Ideally, for a quantitative comparison between the NSR and ECR, such measurements should be performed on the same sample and the NSR data obtained over a wide frequency range (i.e., over a decade or more). The wide frequency range is necessary in order that the activation energy of the NSR correlation time can be determined and compared to that of the ECR time. To the best of our knowledge there are only two superionic glasses that have been studied experimentally in such a detailed manner. One example is the Li chlorolborate glass referenced above on which NSR (Ref. 5) and ECR (Ref. 14) measurements were made in such detail that permitted Tatsumisago, Angell, and Martin to extract all the relaxation characteristics of the data from both techniques and make possible a theoretical interpretation[18,20] in the framework of the coupling model. The other example is the $(Li_2S)_{0.56}(SiS_2)_{0.44}$ glass in the work of Borsa *et al.*[6] A similar glass $(Li_2S)_{0.5}(SiS_2)_{0.5}$ was studied actually earlier by Pradel and Ribes,[22] however there the NSR measurement was not carried out over a wide frequency range. As we shall see the NSR data of Borsa *et al.* taken over a wide frequency range can provide a more accurate determination of NSR characteristics of the superionic glass. A comparison between NSR and ECR properties has not been carried out to the extent allowed by the good quality of this set of experimental data.[6] The purpose of this work is to further exploit this valuable set of experimental data for a more in depth comparison between NSR and ECR, and to bring out the consequences of this comparison by using the coupling model (Refs. 2, 9, 18–20, 23, and 24).

THEORETICAL

In conductivity measurements the dynamical variable probed is the current j and relaxation is determined by the current-current correlation function, $C_\sigma(t) = \langle \mathbf{j}(t)\mathbf{j}(0)\rangle$. On the other hand, in NSR measurements if the ion spin-relaxation mechanism is via magnetic dipole or quadrupolar interactions, the NSR is governed[25] by the correlation function, $C_s(t) = (1/N)\sum_{i\neq j}^{N}\langle F_{ij}^{(q)}(t)F_{ij}^{(q)}(0)\rangle$, where

$$F_{ij}^{(q)}(t) = (q\sqrt{8\pi/15})Y_2(q)\Omega_{ij}/r_{ij}^3 ,$$

where Y is the spherical harmonics, r_{ij} is the distance between two ions, and $q=1,2$. The general practice used to analyze experimental data is to assume[4–18] that the correlation functions all have the stretched exponential functional form,

$$C_U(t) = \exp[-(t/\tau_U^*)^{1-n_U}] , \quad (1)$$

where $U=s$ or σ. Such a practice has a justification from the coupling model[23,24] for relaxation of correlated systems of which the glassy ionic conductors form a special class. Following the general physical principle on which the coupling model is based,[23,24] at sufficiently short times the effects of the mutual interaction are not operative and the relaxation is governed by the independent relaxation rate of a single ion given by $W_0=1/\tau_0$. This single-ion dependent relaxation rate is slowed down to assume the self-similar time dependence of $W_0(\omega_c t)^{-n_U}$ after a characteristic time scale $1/\omega_c$ has been crossed. From this basic result of the coupling model, we obtain the stretched exponential correlation function, Eq. (1) with β_U given by

$$\beta_U=1-n_U \ , \tag{2}$$

together with the relation between the effective correlation time τ_U^* and the independent ion correlation time τ_0 given by

$$\tau_U^*=[(1-n_U)\omega_c^{n_U}\tau_0]^{1/(1-n_U)} \ . \tag{3}$$

If τ_0 is thermally activated and has the form

$$\tau_0=\tau_\infty \exp(E_a/kT) \ , \tag{4}$$

then from the very definition of τ_0 the activation energy E_a must be the true energy barrier that has to be surmounted by a single ion in the elementary step of motion and before correlation (cooperativity) with other ions are considered. It should be independent of the dynamical variable U being probed. In other words the same τ_0 appears in Eq. (3) for all U's. Substituting this expression for τ_0 into Eq. (3) the effective relaxation time has the corresponding form:

$$\tau_U^*=[(1-n_U)\omega_c^{n_U}\tau_\infty]^{1/(1-n_U)}\exp(E_U^*/kT) \ . \tag{5}$$

Its effective activation energy E_U^* is related to the true activation energy barrier through the nonexponentiality index (called the coupling parameter) n_U by the relation

$$E_U^*=E_a/(1-n_U) \ . \tag{6}$$

This feature distinguishes the coupling model and some related models[16,21,26,27] from other models in that the effective energy barrier E_U^* of measured quantities such as dc conductivity, tracer diffusion constant, and NSR correlation time is not the true energy barrier, E_a, that an ion sees when the mutual interactions between ions are switched off. The difference between E_U^* and E_a is caused by the effects of correlation from the presence of other ions. Other theories have identified the effective energy barrier E_U^* but not E_a to be the true energy barrier that a ion has to surmount. These theories exemplified by Ref. 17 as well as conventional wisdom [see Eqs. (7) and (10a) in Ref. 6] also expect the same stretch exponential correlation function, and hence the same stretch exponent β_U, effective relaxation time τ_U^*, and activation energy E_U^*, for all U's. Very recently, Bunde, Maass, and Meyer[21] have found from computer simulations of interacting charged particles in a structurally disordered system, that the exponents β_s and β_σ differ significantly with $\beta_s<\beta_\sigma$. Both this computer simulation result and the pronounced differences in β_U, τ_U^*, and E_U^* between NSR and ECR, established by Tatsumisago, Angell, and Martin[14,15] have severely undermined our confidence in these models and even conventional wisdom. On the other hand in the coupling model, E_a is the true energy barrier and hence it is the same for all U's. As we have already shown in Ref. 18, from the conceptual framework of the coupling model, we have concluded that $\beta_s<\beta_\sigma$. This result together with the predicted relation between E_a and E_U^* given by Eq. (6) explain the large differences in τ_s^* and τ_σ^* with $\tau_s^*\gg\tau_\sigma^*$ at the same temperature and the fact that $E_s^*>E_\sigma^*$. We shall further demonstrate that the products $\beta_\sigma^* E_s^*$ and $\beta_\sigma^* E_\sigma^*$ have the same value, as expected from the coupling model because each of these products is E_a, a true energy barrier.

It has been pointed out that in Ref. 18 that although NSR and ECR both originate from the same ion transport dynamics, they are governed by very different correlation functions. Indeed there is a drastic difference between $C_s(t)$ and $C_\sigma(t)$. The appearance of the r_{ij}^{-3} factor in $C_s(t)$ has the consequence that the contributions from ion pairs at shorter separation distance are weighed more heavily in $C_s(t)$ than in $C_\sigma(t)$. As a result, the effect of mutual interactions between the ions is significantly enhanced in $C_s(t)$ than in $C_\sigma(t)$ and consequently the coupling parameter n_s for NSR will be larger than n_σ, for ECR, i.e.,

$$n_s>n_\sigma \ . \tag{7}$$

In Ref. 18 we have shown how starting from this relation given by (7), the pronounced difference between NSR and ECR observed in the Li chloroborate glass[14] can be quantitatively explained by the coupling model [contained in Eqs. (1)–(6)] using the nonexponentially or coupling parameters n_s and n_σ that have been determined by fitting the shape of the NSR T_1 minimum and the frequency dependence of the electric modulus data, respectively. We shall demonstrate here the same success of the coupling model is also found in Li_2Si-SiS_2.

RESULTS AND DISCUSSION

The NSR and ECR data of the Li chloroborate glass has been analyzed by Tatsumisago, Angell, and Martin and the discrepancies in their relaxation characteristics are summarized here in Table I. We shall come back to

TABLE I. Comparison of ^{7}Li nuclear spin relaxation (NSR) and electrical-conductivity relaxation (ECR) in Li chloroborate glass, $(LiCL)_{0.6}(Li_2O)_{0.5}(B_2O_3)_{1.0}$.

Dynamical variable, U	n_U	$\beta_U\equiv1-n_U$	E_U^* (K)	$(1-n_U)E_U^*$ (K)
s (NSR)[a]	0.65	0.35	7400±200	2590
σ (ECR)[b]	0.50	0.50	5500	2750

[a]Reference 5.
[b]Reference 14.

discuss these pronounced differences observed in Li chloroborate glass together with a similar effect seen in the Li_2S+SiS_2 glasses. First let us summarize the NSR and ECR data of $(Li_2S)_{0.56}(SiS_2)_{0.44}$. Some of the NSR data will be reanalyzed.

The frequency and temperature dependence of ECR and of ^{7}Li NSR rates have been presented in Ref. 6. Both the ECR and NSR experimental data have been analyzed using the stretched exponential correlation function. The results of the analysis have been given in Table I of Ref. 6. The stretch exponents β_s and β_σ are significantly different ($\beta_s=0.35$ and $\beta_\sigma=0.48$). The effective activation energies E_s^* and E_σ^* are also different ($E_s^*=4500+200$ and $E_\sigma^*=4000+50$ K) in accordance with the general rule established before[14,18,20] in the Li chloroborate glass and other glasses. The parameters β_s and E_s^* quoted were obtained by fitting the NSR rate (at constant Larmor frequency) versus reciprocal temperature curves with the stretched exponential correlation function. Although a legitimate procedure, this is not the most accurate way to obtain the relaxation parameters from these data. In fact, in the previous analysis of the Li_2S+SiS_2, advantage has not been taken of an alternative method of determining E_s^* when NSR data taken over a wide range of frequencies are available. It is well known that the NSR rate $1/T_1$ can be calculated from the correlation function $C_s(t)$ via the spectral density function $J(\omega)$ by

$$1/T_1=A\{J(\omega_L)+4J(2\omega_L)\}\ , \tag{8}$$

where

$$J(\omega_L)=\mathrm{Re}\int_0^\infty C_s(t)\exp(-i\omega_L t)dt \tag{9}$$

and A is the coupling constant. Alternatively this expression can be transformed to

$$1/T_1=A\{E''(\omega_L)/\omega_L+4E''(2\omega_L)/2\omega_L\}\ , \tag{10}$$

where

$$E''(\omega_L)=\int_0^\infty dt\exp(-i\omega_L t)(-dC_s(t)/dt)\ . \tag{11}$$

If the correlation function is a function only of the dimensionless scaled time t/τ_s^* as in the case of the stretched exponential given by Eq. (1), then it is easy to show that E'' is a function of the product $\omega_L\tau_s^*$ only. Making use of this fact, we can rewrite the expression given by Eq. (10) as

$$1/T_1=A\{E''(\omega_L\tau_s^*)/\omega_L\tau_s^*+4E''(2\omega_L\tau_s^*)/2\omega_L\tau_s^*\}\tau_s^*\ . \tag{12}$$

For any Larmor frequency $1/T_1$ given by Eq. (12) assumes the maximum value, $(1/T_1)_{\max}$, at a temperature $T_{\max}$ when $\omega_L\tau_s^*$ is equal to a constant h of order of unity. The exact value of the constant depends on the value of the stretch exponent. Hence, from Eq. (12) we obtain the relation

$$(1/T_1)_{\max}=A\{E''(h)/h+4E''(2h)/2h\}\times\tau_\infty^*\exp(E_s^*/T_{\max})\ . \tag{13}$$

An Arrhenius plot of $(1/T_1)_{\max}$ against $T_{\max}$ will enable us to determine E_s^*. This method was known and applied before to NSR.[23,9]

The extensive NSR rate measurements performed on $(Li_2S)_{0.56}(SiS_2)_{0.44}$ over a decade in Larmor frequencies makes the situation ideal to apply this method for an accurate determination of E_s^*. The large number of experimental points enables the locations of the $1/T_1$ maxima, $[T_{\max},(1/T_1)_{\max}]$, to be determined with good precision. The straight line drawn in Fig. 1 is a least-squares fit to the data obtained at 4, 7, 12.2, and 40 MHz. The slope of this line determines the effective activation energy E_s^* of the ^{7}Li NSR correlation time τ_s^*. The value obtained is 48.60 kJ/mol, or equivalently 5845 K in temperature units, and entered into Table II. This value of E_s^* should be more accurate than that obtained from using the stretch exponential to fit the $1/T_1$ experimental data as a function of reciprocal temperature at constant ω_L, a method which becomes reliable for determining E_s^* only if $1/T_1$ data points taken on the high-temperature side of the maximum have attained[9,23] the limiting dependence of

$$1/T_1\sim\tau_s^*(\omega_L)^0\ . \tag{14}$$

This condition for reliability is generally difficult to fulfill because a glass transition intervenes at higher temperature to limit the temperature range within which data can be taken. Even for the superionic glass considered here the asymptotic behavior (14) has not been attained by the experimental data (see Fig. 3 of Ref. 6 or Fig. 1 in this paper).

Equation (10) indicates also that $(1/T_1)_{\max}$ should be inversely proportional to ω_L. This useful additional relation written out explicitly as

$$(1/T_1)_{\max}\propto\omega_L^{-1} \tag{15}$$

can be checked. In Fig. 2 we plot $(1/T_1)_{\max}$ against ω_L.

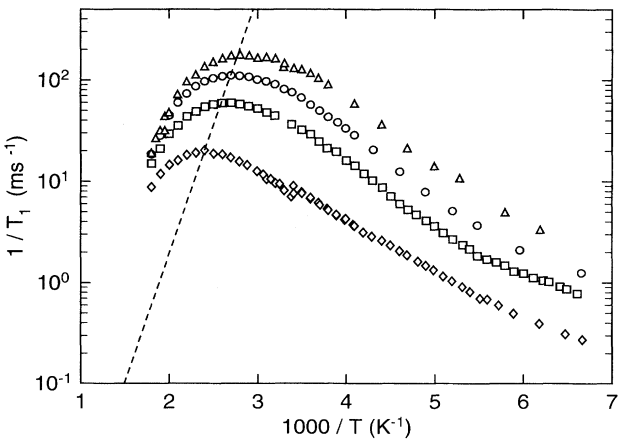

FIG. 1. Experimental data of ^{7}Li spin-lattice relaxation rate in $(Li_2S)_{0.56}(SiS_2)_{0.44}$ from Borsa *et al.* (Ref. 6). (a) Logarithm of the relaxation rates measured at 4.0, 7.0, 12.2, and 40.0 MHz as a function of reciprocal temperature, $1000/T$. (b) Dashed line is drawn through the four maxima of the $(1/T_1)$ data at constant Larmor frequencies (see text).

TABLE II. Comparison between ^{7}Li nuclear spin relaxation (NSR) and electrical-conductivity relaxation in $(Li_2S)_{0.56}(SiS_2)_{0.44}$ glass[a].

Dynamical variable, U	n_U	$\beta_U \equiv 1-n_U$	E_U^* (K)	$(1-n_U)E_U^*$ (K)
s (NSR)[a]	0.65	0.35	5845[b]	2045.8
σ (ECR)[a]	0.48	0.52	3911 (from electric modulus)	2033.7
			4000 (from dc conductivity)	2080.0

[a]Reference 6.
[b]Determined in this work (see Figs. 1 and 3).

The slope determined by least-squares fit to the data is -0.956, which is close to the expected value of -1.0. Thus this cross check of the frequency dependence of $(1/T_1)_{\max}$ should enhance the confidence in the value of the activation energy E_s^* determined.

With the nonexponentialty parameter β_U and the activation energy E_U^* of τ_U^* having been determined for NSR ($U=s$) and for ECR ($U=\sigma$), their values are entered into Table II. It has already been found that $1/T_1$ and the electric modulus[11,13] $M^*(\omega)$ have to be fitted with different values of the stretch exponent as can be seen in Table II. The difference between these two exponents is quite significant with β_s being smaller:

$$\beta_s < \beta_\sigma \ . \tag{16}$$

In Fig. 3 we plot the most probable conductivity relaxation time τ_σ^* defined from the peak frequency of the imaginary part of the electric modulus M'' according to

$$\tau_\sigma^* = 1/2\pi f_{\max} \tag{17}$$

together with NSR correlation time τ_s^* obtained using the usual assumption that, at the $1/T_1$ maximum, the relation $\omega_L \tau_s^* \simeq 1$ holds. It is clear from Fig. 3 that there is a rather large difference between the time scales of the two processes, not only in the values of the correlation time at

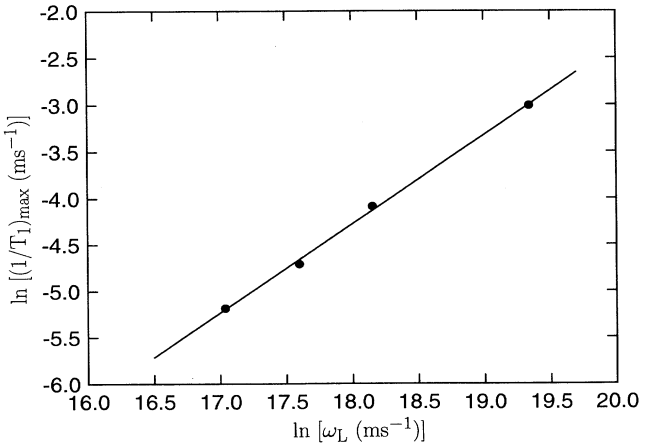

FIG. 2. A ln-ln plot of the value of the $(1/T_1)$ maximum against Larmor frequency ω_L.

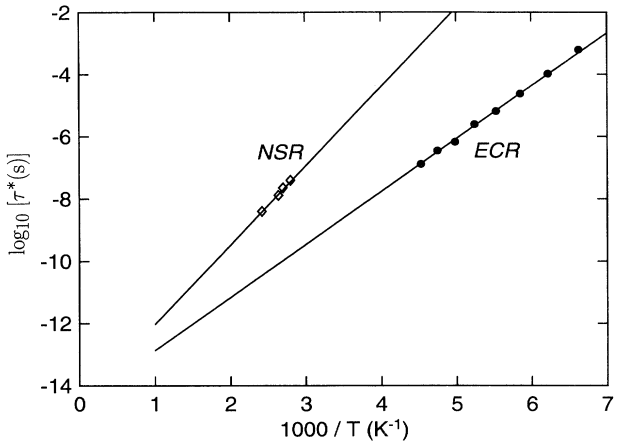

FIG. 3. Arrhenius plot of the nuclear spin-relaxation correlation time τ_s^* (open diamonds) and the conductivity relaxation time τ_σ^* (filled circles). The different slopes of the two straight lines drawn through the data indicate the large difference between the two activation energies.

any chosen temperature, but also in their temperature dependences, i.e.,

$$\tau_s^*(T) \gg \tau_\sigma^*(T) \ , \tag{18}$$

and

$$E_s^* > E_\sigma^* \ . \tag{19}$$

We shall now discuss the immense physical implications these results in $(Li_2S)_{0.56}(SiS_2)_{0.44}$ and in $(LiCl)_{0.6}(Li_2O)_{0.5}(B_2O_3)$ (summarized in Table I) have in the search for the correct description of the ion transport dynamics. First of all, these two sets of results are pointing to the fact that there are pronounced differences between NSR and ECR. The large discrepancy between E_s^* and E_σ^*, between β_s and β_σ, and between τ_s^* and τ_σ^* at any chosen temperature in both glasses indicate that these differences are real and general. These anomalies found here, like their analogs in many other fields of scientific research, are "... the real guide to the truth."[28] They play important roles in the identification among many possible theories the correct description of the ionic transport dynamics. At the outset, theories that predict or require τ_s^* and τ_σ^* to be the same contradict experimental fact (Fig. 3 here and Fig. 4 in Ref. 14 and Tables I and II here). As has already been mentioned earlier in passing, the large difference between E_s^* and E_σ^* contradicts many theories of ionic conductivity relaxation (ECR) which identify the dc conductivity activation energy or equivalently E_σ^* to be the true energy barrier seen by an ion in the glass. This is because theories of ECR, which equate E_σ^* to the true energy barrier, when extended to treat NSR, in all likelihood will have to do the same in NSR, i.e., equating E_s^* to the same true energy barrier, thus E_s^* is equal to E_σ^* which contradicts the experimental findings. The experimentally observed large discrepancy between E_s^* and E_σ^* will pose a problem even

in a theoretical vacuum if either one of these quantities were identified with the true single-ion energy barrier. Such an identification of one of the activation energies with the true energy barrier will impose inextricable constraints that make an explanation of the other differing activation energy extremely difficult if not impossible.

The coupling model distinguishes itself in identifying neither E_s^* nor E_σ^*, but the products $\beta_s E_s^*$ and $\beta_\sigma E_\sigma^*$ to be the true single-ion activation energy barrier, which earlier [Eq. (4)] we have denoted by E_a:

$$\beta_s E_s^* = \beta_s E_\sigma^* = E_a \ . \tag{20}$$

The dependence of the stretch exponent β_U of the correlation function $C_U(t)$ on the dynamical variable U being probed is expected from the conceptual and theoretical basis of the coupling model. In fact we have advanced[18] physical arguments to justify the inequality (16) between the two exponents for ECR and NSR. Although it is impossible at this time to calculate these exponents for a glass as complex as $(Li_2S)(SiS_2)$, they can be determined by fitting the shapes of the $1/T_1$ curves when plotted against reciprocal temperature and the dispersion of the electric modulus $M^*(\omega)$ curves when plotted against the logarithm of frequency. The values of the stretch exponents in Tables I and II have been obtained in this way. On the other hand, the activation energies E_s^* and E_σ^* are obtained from the shifts of the $1/T_1$ maximum with Larmor frequency (see Fig. 1) and temperature dependence of the dc conductivity (see Fig. 2 in Ref. 6), respectively. The significant difference between the experimental activation energies follows from Eq. (6) as an immediate consequence of the difference between the corresponding stretch exponents. The acid test of the coupling model comes with Eq. (20). In Tables I and II we form the products that appear in Eq. (20). Remarkably, as can be seen by inspection of these tables, the products $\beta_s E_s^*$ and $\beta_\sigma E_\sigma^*$ are equal in each superionic glass within the experimental errors involved in the determination of the parameters from experimental data. The constancy of the product $\beta_U E_U^*$ as predicted by Eq. (20) validates its identification as the true single-ion energy barrier. There are other experimental data of different nature from the ones discussed here that have led also to the same conclusion. These include the quasielastic neutron-scattering data in fast-ion conductors,[29] the NSR data of many alkali-oxide glasses,[2,29] which are poor ionic conductors, a calculation of the single-ion energy barrier from structural information obtained from extended x-ray-absorption fine structure,[27] and a recent direct observation of the true energy barrier by dielectric loss spectroscopy at low temperature in a lithium alumino-silicate glass ceramic by Bohmer *et al.*[30] Evidence from this work and previous works in other ionic glasses together with the implications of this evidence on ion transport dynamics discussed here have enhanced our confidence in identifying $\beta_U E_U^*$ to be the true energy barrier for the motion of an ion.

ACKNOWLEDGMENT

K.L.N. was supported in part by ONR Contract No. N0001493WX24011.

[1]D. Brinkman, Solid State Ionics **5**, 53 (1981).
[2]G. Balzer-Jöllenbeck, O. Kanert, H. Jain, and K. L. Ngai, Phys. Rev. B **39**, 6071 (1989); O. Kanert, R. Kühler, S. Estalji, K. L. Ngai, and H. Jain, in *The Physics of Non-Crystalline Solids,* edited by L. D. Pye, W. C. LaCourse, and H. J. Stevens (Taylor and Francis, London, 1992), p. 178.
[3]A. Pradel and M. Ribes, J. Non-Cryst. Solids **131-133**, 1063 (1991).
[4]S. Martin, Mater. Chem. Phys. **23**, 225 (1989), and references therein.
[5]M. Trunnell, D. R. Torgeson, S. W. Martin, and F. Borsa, J. Non-Cryst. Solids **139**, 257 (1992).
[6]F. Borsa, D. R. Torgeson, S. W. Martin, and H. K. Patel, Phys. Rev. B **46**, 795 (1992).
[7]P. Heitjans, W. Faber, and A. Schirmer, J. Non-Cryst. Solids **131-133**, 1053 (1991).
[8]S. H. Chung, K. R. Jeffery, J. R. Stevens, and L. Borjesson, Phys. Rev. B **41**, 6154 (1990).
[9]K. L. Ngai, Solid State Ionics **5**, 27 (1981).
[10]A. Bunde, P. Maass, and M. Meyer, Physica A **191**, 433 (1992).
[11]P. B. Macedo, C. T. Moynihan, and R. Bose, Phys. Chem. Glasses **13**, 171 (1972).
[12]B. Munro, M. Schrader, and P. Heitjans, Ber. Bunsenges. Phys. Chem. **96**, 1718 (1992).
[13]C. A. Angell, Chem. Rev. **90**, 523 (1990).
[14]M. Tatsumisago, C. A. Angell, and S. W. Martin, J. Chem. Phys. **97**, 6968 (1992).
[15]C. A. Angell, Annu. Rev. Phys. Chem. **172** (1992).
[16]K. Funke, Prog. Solid State Chem. **22**, 111 (1993).
[17]S. R. Elliott and A. P. Owens, Phys. Rev. B **44**, 47 (1991).
[18]K. L. Ngai, J. Chem. Phys. **98**, 6424 (1993).
[19]K. L. Ngai, R. W. Rendell, and H. Jain, Phys. Rev. B **30**, 2133 (1984).
[20]K. L. Ngai, Solid State Ionics **61**, 345 (1993).
[21]A. Bunde, P. Maass, and M. Meyer, in *Proceedings of the International Conference on Defects in Insulating Materials,* edited by O. Kanert and M. Spaeth (World Scientific, Singapore, 1993), p. 295; (unpublished).
[22]A. Pradel and M. Ribes, J Non-Cryst Solids **131-133**, 1041 (1991).
[23]K. L. Ngai, Comments Solid State Phys. **9**, 127 (1979); **9**, 141 (1980).
[24]K. L. Ngai, S. L. Peng, and K. Y. Tsang, Physica A **191**, 523 (1992).
[25]A. Abragam, *The Principles of Nuclear Magnetism* (Clarendon, Oxford, 1962).
[26]P. Maass, J. Petersen, A. Bunde, W. Dieterich, and H. E. Roman, Phys. Rev. Lett. **66**, 52 (1991).
[27]G. N. Greaves and K. L. Ngai, in *Proceedings of the International Conference on Defects in Insulating Materials,* edited by O. Kanert and J.-M. Spaeth (World Scientific, Singapore, 1993), p. 53.
[28]P. W. Anderson, Physics Today **43** (February), 9 (1990).
[29]K. L. Ngai and O. Kanert, Solid State Ionics **53-56**, 936 (1992).
[30]R. Böhmer, G. Gerhard, F. Drexler, A. Loidl, K. L. Ngai, and W. Pannhorst, J. Non-Cryst. Solids **155**, 189 (1993).